Mon. Not. R. Astron. Soc. **388,** L84–L88 (2008) doi:10.1111/j.1745-3933.2008.00504.x

Testing reionization with gamma-ray burst absorption spectra

S. Gallerani,[1⋆] R. Salvaterra,[2] A. Ferrara[1] and T. Roy Choudhury[3]

[1] *SISSA/International School for Advanced Studies, via Beirut 2-4, 34014 Trieste, Italy*
[2] *Dipartimento di Fisica G. Occhialini, Università degli Studi di Milano Bicocca, Piazza della Scienza 3, I-20126 Milano, Italy*
[3] *Institute of Astronomy, Madingley Road, Cambridge CB3 OHA*

Accepted 2008 May 22. Received 2008 May 16; in original form 2007 October 4

ABSTRACT

We propose to study cosmic reionization using absorption-line spectra of high-redshift gamma-ray burst (GRB) afterglows. We show that the statistics of the dark portions (gaps) in GRB absorption spectra represent exquisite tools to discriminate among different reionization models. We then compute the probability to find the largest gap in a given width range $[W_{\rm max}, W_{\rm max} + {\rm d}W]$ at a flux threshold $F_{\rm th}$ for burst afterglows at redshifts $6.3 \leq z \leq 6.7$. We show that different reionization scenarios populate the $(W_{\rm max}, F_{\rm th})$ plane in a very different way, allowing to distinguish among different reionization histories. We provide here useful plots that allow a very simple and direct comparison between observations and model results. Finally, we apply our methods to GRB 050904 detected at $z = 6.29$. We show that the observation of this burst strongly favours reionization models which predict a highly ionized intergalactic medium at $z \sim 6$, with an estimated mean neutral hydrogen fraction $x_{\rm H\,I} = 6.4 \pm 0.3 \times 10^{-5}$ along the line of sight towards GRB 050904.

Key words: intergalactic medium – large-scale structure of Universe – gamma-rays: bursts.

1 INTRODUCTION

In the last few years, our knowledge of the high-z Universe and in particular of the reionization process has been enormously increased mainly owing to the observation of quasars by the Sloan Digital Sky Survey (SDSS) survey (Fan 2006) and cosmic microwave background (CMB) data (Hinshaw et al. 2007; Page et al. 2007). Long gamma-ray bursts (GRB) may constitute a complementary way to study the reionization process avoiding the proximity effects and possibly probing even larger redshifts. This has now become clear after the detection of five GRBs at $z \gtrsim 5$, over a sample of about 200 objects observed with the *Swift* satellite (Gehrels et al. 2004). The current record holder is GRB 050904 at $z = 6.29$ (Tagliaferri et al. 2005; Kawai et al. 2006). Totani et al. (2006) have used this object to constrain the ionization state of the intergalactic medium (IGM) at high redshift by modelling its optical afterglow spectrum. They report the evidence that the IGM was largely ionized already at $z = 6.3$. The best-fitting neutral hydrogen fraction is consistent with zero with upper limit $x_{\rm H\,I} < 0.17$ (<0.6) at 68 per cent (95 per cent) CL.

Several authors (Natarajan et al. 2005; Bromm & Loeb 2006; Daigne, Rossi & Mochkovitch 2006; Salvaterra et al. 2007) have computed the number of high-z GRBs detectable by *Swift*. In spite of model details, all these different studies consistently predict that a non-negligible fraction (up to ∼10 per cent) of all observed GRBs should lie at very high redshift. On the basis of these results, several GRBs at $z \geq 6$ should be observed by *Swift* in near future. Depending on the *Swift*/BAT trigger sensitivity and on model details, Salvaterra & Chincarini (2007) found that ∼2–8 GRBs can be detected above this redshift during every year of mission. From the observational point of view, Ruiz-Velasco et al. (2007) find that the fraction of *Swift* GRBs at $z > 6$ should not exceed the conservative upper limit of 19 per cent. Moreover, future X-ray and Gamma-ray missions will increase rapidly the sample of high-z GRBs, possibly up to $z \sim 10$ (Salvaterra et al. 2008). Once detected, spectroscopic follow-up observations of high-z GRBs require a rapid trigger of 8 m, ground-based telescopes. This can be done by pre-selecting reliable candidates on the basis of some promptly available information provided by *Swift*, such as burst duration, photon flux, the lack of detection in the UVOT V band, and the low Galactic extinction (Campana et al. 2007; Salvaterra et al. 2007). We note that cosmological time dilation helps keeping the flux bright, since observations will sample the afterglow early phases, even a few days after trigger.

The spectra of high-redshift sources (as QSOs and GRBs) bluewards of the Lyα are characterized by dark portions (gaps) produced by intervening neutral hydrogen along the line of sight. The use of various gap statistics in QSO spectra has been recently recognized as a very powerful tool to constrain the IGM ionization state (Paschos & Norman 2005; Fan et al. 2006; Gallerani, Choudhury & Ferrara 2006, hereafter G06; Gallerani et al. 2007, hereafter G07). For example, by comparing the statistics of these spectral features in a sample of 17 observed QSOs with Lyα forest simulations, G07

⋆E-mail: galleran@sissa.it

concluded that the H I fraction, $x_{\rm H\,I}$, evolves smoothly from $10^{-4.4}$ at $z = 5.3$ to $10^{-4.2}$ at $z = 5.6$, with a robust upper limit $x_{\rm H\,I} < 0.36$ at $z = 6.3$. These results encourage the application of such analysis to GRBs. There are several advantages promised by such an attempt. First, GRBs are soon expected to be found at redshifts higher than those typical of QSOs; secondly, and contrary to the massive hosts of QSOs, they reside in 'average' cosmic regions only marginally affected by local ionization effects or strong clustering; finally, they are bright and their afterglow spectra closely follow a power law, making continuum determination much easier.

In agreement with the *WMAP3* results (Spergel et al. 2007), we assume a flat universe with $\Omega_{\rm m} = 0.24, \Omega_\Lambda = 0.76, \Omega_{\rm b}\,h^2 = 0.022, h = 0.73$. The parameters defining the linear dark matter power spectrum are $n = 0.95$, $\mathrm{d}n/\mathrm{d}\ln k = 0, \sigma_8 = 0.82$. Mpc are physical unless differently stated.

2 GRB EMISSION PROPERTIES

We have built a synthetic GRB afterglow emission spectrum starting from the observed spectral energy distribution and time evolution of the most distant GRB detected up-to-now, i.e. GRB 050904 at $z = 6.29$ (Tagliaferri et al. 2005; Kawai et al. 2006). The unabsorbed afterglow spectrum of GRB 050904 can be parametrized as $F(\nu) \propto \nu^\alpha t^\beta$, with $\alpha = -1.25^{+0.15}_{-0.14}$ (Tagliaferri et al. 2005; Haislip et al. 2006). The observed temporal decay up to 0.5 d from burst is well described by a power-law index of -1.36 ± 0.06, followed by a plateau phase with $\beta = -0.82 \pm 0.15$ lasting until 2.6 d after burst (Haislip et al. 2006). The further afterglow evolution can be described assuming $\beta = -2.4 \pm 0.4$ (Tagliaferri et al. 2005). Finally, we normalize the intrinsic GRB 050904 optical spectrum in order to reproduce the flux of $\sim$18 μJy as measured at 1 d from burst in the *J* band (Haislip et al. 2006). Although we have experimented with other choices to explore the model sensitivity to redshift, we will mostly show results for GRBs located in the range $6.3 \leq z \leq 6.7$, which appears to be crucial to properly follow the latest (i.e. overlap) phases of reionization history. From the observed afterglow spectral evolution of GRB 050904, we compute the rest-frame spectrum between Lyα (1215.67 Å) and Lyβ (1025.72 Å).

3 ABSORPTION SPECTRA

The ultraviolet radiation emitted by a GRB can suffer resonant Lyα scattering as it propagates through the intergalactic neutral hydrogen. In this process, photons are removed from the line of sight (LOS) resulting in an attenuation of the source flux, the so-called Gunn–Peterson (GP) effect. Thus, the observed flux $F_{\rm obs}$ is given by $F_{\rm obs} = F(\nu)\,\mathrm{e}^{-\tau_{\rm GP}}$, where $\tau_{\rm GP}$ is the GP optical depth. To simulate the $\tau_{\rm GP}$ distribution, we use the method described by G06 and further revised in G07, whose main features are summarized as follows. Mildly non-linear density fluctuations giving raise to spectral absorption features in the intergalactic medium (IGM) are described by a lognormal distribution, which has been shown to fit observational data at redshifts $1.7 < z < 5.8$ (Becker, Rauch & Sargent 2007). For a given IGM equation of state (i.e. temperature–density relation), the mean H I fraction, $x_{\rm H\,I}$, can be computed from photoionization equilibrium (an excellent approximation under the prevailing physical conditions) as a function of the baryonic overdensity, $\Delta \equiv \rho/\bar{\rho}$, and photoionization rate, Γ, due to the ultraviolet background radiation field. These quantities must be determined from a combination of theory and observations; here, we follow the approach of Choudhury & Ferrara (2006, CF06 hereafter). Their study allows for three types of ultraviolet ionizing photons: QSOs, Pop II and Pop III stars. As the contribution of Pop III stars is negligible for the redshift of interest here, we neglect this type of sources. The CF06 model contains two free parameters: (i) the star formation efficiency f_* and (ii) the escape fraction $f_{\rm esc}$ of ionizing photons from galaxies. These are calibrated by a maximum-likelihood procedure to a broad data set, including the redshift evolution of Lyman-limit systems, Lyα and Lyβ GP optical depths, electron scattering optical depth, cosmic star formation history and number counts of high-redshift sources.

Currently, the available data can be explained by two different reionization histories, corresponding to different choices of the free parameters: (i) an early reionization model (ERM) ($f_* = 0.1$; $f_{\rm esc} = 0.07$) and (ii) a late reionization model (LRM) ($f_* = 0.08$; $f_{\rm esc} = 0.04$). These two models bracket the range of possible reionization histories. For example, models in which reionization occurs earlier (later) than in the ERM (LRM) would overproduce the electron scattering (GP) optical depth. The global properties of the two reionization models are shown in fig. 1 of G07, so we do not report them here. It suffices to say that in the ERM the volume filling factor of ionized regions, $Q_{\rm H\,II} = V_{\rm H\,II}/V_{\rm tot} = 1$ at $z \leq 7$; in the LRM $Q_{\rm H\,II}$ evolves from 0.65 to unity in the redshift range 7.0–6.0, implying that the reionization is still in the pre-overlap stage at $z \geq 6$. Both ERM and LRM by construction provide an excellent fit to the mean neutral hydrogen fraction evolution experimentally deduced from the GP test. Having selected all the necessary physical evolutionary properties of the most likely reionization histories, we can now describe how we plan to use GRBs to discriminate between them.

4 REIONIZATION TESTS

The main idea we propose in this paper is to exploit the statistics of the transmissivity gaps imprinted by the intervening IGM neutral hydrogen on the otherwise smooth power-law spectrum of high-redshift GRBs. On general grounds, we expect that at any given redshift, but particularly above $z = 6$, where differences become more marked, the value of $x_{\rm H\,I}$ is higher in the LRM than in the ERM. As a result, if reionization completes later, absorption spectra are characterized by wider and more numerous gaps, defined as contiguous regions of the spectrum with observed flux lower than a given flux threshold over a rest-frame wavelength interval larger than 1 Å. Moreover, the level of neutral hydrogen fluctuations along the LOS to the GRB differs in the two models: in principle, the GRB flux decay could be used as a tunable high-pass filter which allows to study the growth of gaps with time. As the time after the burst increases, the gaps become larger. In fact, the progressive fading of the unabsorbed afterglow produces a corresponding attenuation of the observed flux, as can be seen from Fig. 1. As the flux falls below the flux threshold $F_{\rm th}^{\rm obs}$ (thin black horizontal lines), the transmission windows disappear, causing the gaps to expand. The thick dashed cyan line shows the largest gap ($W_{\rm max}$) along the LOS; the largest gap width (LGW) increases as the GRB flux fades. However, in practice, the analysis of the LGW time evolution can be equivalently applied at a fixed time after the burst to the transmitted flux $F_{\rm transm} = F_{\rm obs}/F(\nu)$ varying the threshold[1] $F_{\rm th}$.

We have derived the evolution of the LGW found in synthetic absorption spectra varying the flux threshold used to define gaps. Suppose that a GRB is observed at a given redshift $z_{\rm GRB}$. We can then ask what is the probability that in its afterglow spectrum the

[1] Note that we define $F_{\rm th}^{\rm obs}$ as the threshold which defines gaps in the observed flux and $F_{\rm th}$ in reference to the transmitted one.

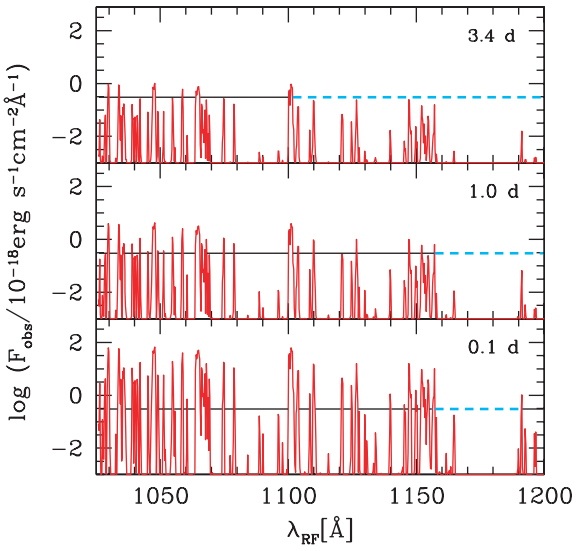

Figure 1. Synthetic absorption spectra at different times after the burst ($t = 0.1$, 1.0, 3.4 d from the bottom panel to the top panel) of a GRB at $z = 6.3$, for the ERM. The thin black horizontal lines denote the flux threshold $F_{\rm th}^{\rm obs}$ used to define gaps. The thick dashed cyan lines show the largest dark gap along each lines of sight.

largest gap, defined by $F_{\rm th}$, is found within a given width range[2] $[W_{\rm max}, W_{\rm max} + {\rm d}\,W]$. We can draw this probability from our model by analysing a large number of synthetic spectra corresponding to different GRB redshifts $z_{\rm GRB}$ and counting the number of LOS having the largest gap in the given range, varying the $F_{\rm th}$ between 0 and 1. Clearly, in real cases, a minimum threshold $F_{\rm th,min}$ is set by the noise associated to the spectrum.

We have computed this statistics for afterglow spectra of GRBs with $6.3 < z_{\rm GRB} < 6.7$. In fact, according to the most recent estimates involving the lower trigger sensitivity, the *Swift* mission is expected to increase the sample of high-z GRBs, possibly up to $z \sim 10$ (Salvaterra et al., in preparation).

We show the resulting largest gap probability isocontours in Fig. 2 for $z_{\rm GRB} = 6.3$ (top panels), $z_{\rm GRB} = 6.5$ (middle panels) and $z_{\rm GRB} = 6.7$ (bottom panels); the left-hand (right) panels refer to the ERM (LRM) case. We use 300 LOS in order to ensure statistical convergence of the results. The isocontours correspond to a probability of 5, 10 and 40 per cent. The differences caused by the two different reionization histories are striking, since the ERM and LRM populate the $(W_{\rm max}, F_{\rm th})$ plane in a very different way, as shown in Fig. 2. For example, at $z_{\rm GRB} = 6.3$, the probability to find the largest gap with $W_{\rm max} = 50$ Å for $F_{\rm th} = 0.1$, is ≈40 per cent, in the ERM, while it is only of the ≈5 per cent in the LRM, being most of the largest gaps wider than 50 Å.

Moreover, in the LRM the width of the gaps is a factor of ≈2 times wider than in the ERM. In particular, for $z_{\rm GRB} = 6.5$ and $F_{\rm th} = 0.2$, we find that in the ERM $40 \lesssim W_{\rm max} \lesssim 170$ Å, while in the LRM, gaps are mostly larger than 80 Å, for the same value of the flux threshold.

Finally, in the ERM the LOS becomes completely dark for flux threshold values higher than in the LRM case, as a consequence of the higher transmitted flux predicted by the former. For example, at $z = 6.7$, in the ERM (LRM) the gap size is equal to the simulated LOS length (≈190 Å) for $F_{\rm th} \approx 0.4$ (0.15).

[2] In this work, we assume d $W = 20$ Å.

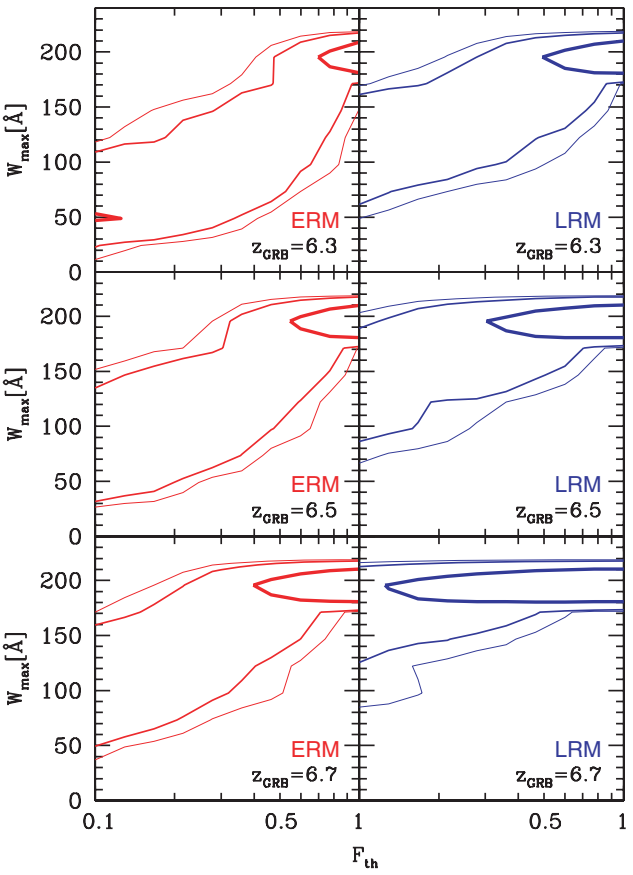

Figure 2. Isocontours of the probability that the afterglow spectrum of a GRB at redshift $z_{\rm GRB}$, contains a largest gap of size in the range $[W_{\rm max}, W_{\rm max} + {\rm d}W]$, with ${\rm d}W = 20$ Å for a flux threshold $F_{\rm th}$. The left-hand (right) panel shows the results for the ERM (LRM). The top (middle, bottom) panel shows the results for $z_{\rm GRB} = 6.3$ (6.5, 6.7). The isocontours correspond to probability of 5, 10 and 40 per cent.

The results point also towards two very important, and potentially interesting, redshift-dependent features, both related to the thickening of the Lyα forest, which becomes on average more neutral towards higher redshifts. First, there is an overall shift towards larger $W_{\rm max}$ values of both ERM and LRM curves from $z_{\rm GRB} = 6.3$ to 6.7. Secondly, the rate at which the gap width grows and saturates with $F_{\rm th}$ strongly correlates with redshift.

Thus, the analysis of the largest gap evolution with the flux threshold shows that it is easier to discriminate among different reionization histories using the highest redshift available sample of GRBs.

Fig. 2 allows a straightforward comparison between data and model results. In practice, information on the reionization history from a $z > 6$ GRB can be easily extracted through the following steps: (i) from the J band afterglow flux, F_J, extrapolate the continuum as $F(\nu) = F_J(\nu/\nu_J)^\alpha$; (ii) compute the transmitted flux $F_{\rm transm} = F_{\rm obs}/F(\nu)$; (iii) Determine the LGW in $F_{\rm transm}$, varying $F_{\rm th}$ in $[F_{\rm th,min}$;1] and (iv) compare the result with Fig. 2. This simple procedure will allow to discriminate between different reionization scenarios.

5 THE CASE OF GRB 050904

We apply the LGW analysis to the observed flux of the GRB 050904, whose spectrum has been obtained 3.4 d after the burst (Kawai et al.

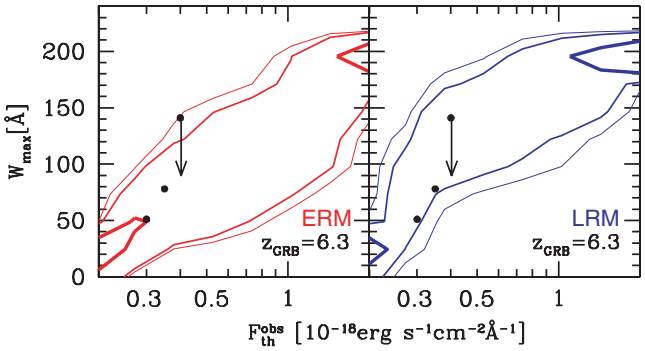

Figure 3. Isocontours of the probability that the afterglow spectrum associated with a GRB at redshift $z_{\rm GRB} = 6.3$, contains a largest gap of size in the range $[W_{\rm max}, W_{\rm max} + {\rm d}W]$, with ${\rm d}W = 20$ Å, for a flux threshold $F_{\rm th}$. The left-hand (right) panel shows the results for the ERM (LRM). The isocontours correspond to probability of 5, 10 and 40 per cent. The black points indicate the position in the $(W_{\rm max}, F_{\rm th}^{\rm obs})$ plane of GRB 050904. The point with arrow means that the gap size should be considered as an upper limit, since the corresponding dark region could be affected by the presence of a DLA (Kawai et al. 2006).

2006). For a fair comparison with observations, simulated spectra have been convolved with a Gaussian of full width at half-maximum (FWHM) = 300 km s^{-1}, providing $R = 1000$, and then rebinned to a resolution of $R = 600$. Finally, we add noise to the simulated data such that the flux F in each pixel is replaced by $F + G(1)\,\sigma_n$, where $G(1)$ is a Gaussian random deviate with zero mean and unit variance, and $\sigma_n = 0.05$ is almost the mean noise rms deviation, observed in the GRB 050904 spectrum by Kawai et al. (2006).

In this work, the lower flux threshold value that we use is $F_{\rm th,min}^{\rm obs} = 0.3 \times 10^{-18}$ erg s^{-1} cm^{-2} Å^{-1} which is $\geq 3\sigma_n$. Such conservative choice of $F_{\rm th}^{\rm obs}$ excludes the possibility that the widths of the gaps are underestimated because of some spurious transmission peaks. For $F_{\rm th}^{\rm obs} = (0.30; 0.35; 0.40) \times 10^{-18}$ erg s^{-1} cm^{-2} Å^{-1}, the observed largest dark gaps sizes are $W_{\rm max} = (51; 78; 141)$ Å, respectively, in the GRB rest frame. These values refer to the dark regions extending in the observed wavelength region ~[7850–8220]; [7850–8420] and [7850–8874] Å, respectively. It is worth noting that the third wavelength range contains the spectral region immediately blueward the Lyα emission, which could be affected by the presence of a damped lyman α (DLA), as claimed by Kawai et al. (2006). Thus, the corresponding quoted size for the dark gap should be consider as an upper limit.

The black filled circles in Fig. 3, corresponding to the values of $W_{\rm max}$ and $F_{\rm th}^{\rm obs}$ for GRB 050904, show that the ERM is favoured by the data. In particular, the probability to find a largest gap of $W_{\rm max} \approx 51$ Å, for $F_{\rm th}^{\rm obs} = 0.30 \times 10^{-18}$ erg s^{-1} cm^{-2} Å^{-1} is ≈40 per cent if reionization occurred early, i.e. almost half of the LOS contains a largest gap of this size for a burst with the redshift and flux of GRB 050904. Such probability drops for a late reionization model to ~10 per cent clearly indicating that in this scenario the GRB 050904 observation represents a much rarer event. Moreover, in the ERM, the probability to find a largest gap of $W_{\rm max} \approx 78$ Å, for $F_{\rm th}^{\rm obs} = 0.35 \times 10^{-18}$ erg s^{-1} cm^{-2} Å^{-1} is almost three times the LRM one (27 versus 10 per cent). Finally, for the third observed point the LRM appears to be more probable than the ERM by a factor of 27:5. This value should be considered an upper limit, since the third point has been obtained analysing a spectral region which could be affected by a DLA contamination (Kawai et al. 2006). For this reason, the corresponding gap size should be smaller than 141 Å, thus being more consistent with ERM predictions, as the other observational data. Without taking into account the latter observed point, we find that the ERM is 11 times more probable than the LRM; if such data point is included, the above vantage factor reduces to 2. We have checked the impact of uncertainties on the continuum flux by varying its slope within the quoted error on α (see Section 2). We have found that the results shown in Fig. 3 are negligibly affected.

Our results are due to the fact that many, relatively large, opaque stretches are present in the IGM at $z = 6.3$ for the LRM, resulting in an average large $W_{\rm max}$. In the case of ERM, reionization is almost complete already at $z \sim 7$ and smaller largest gaps are expected at the redshift of GRB 050904.

Although a large sample of high-redshift GRBs is required before we conclude that a model in which reionization ended by $z \approx 7$ is favoured by the data, the discriminating power of the proposed method is already apparent.

5.1 Neutral hydrogen measurements

We have compared the gap statistics as predicted by two different reionization models. At $z = 6$, the ERM predict a mean neutral hydrogen fraction $x_{\rm H\,I} \sim 10^{-4}$, while in the LRM $x_{\rm H\,I} \sim 0.03$. As shown in the previous sections, the gap statistics are sensitive to the neutral hydrogen amount along the LOS to the background source. Thus, we can exploit the better agreement of the ERM predictions with observed data to provide a measurement of the neutral hydrogen fraction $x_{\rm H\,I}$ along the LOS to the GRB 050904. To this aim, from the ERM sample used in the analysis, we select those LOS whose largest gap is consistent with observations. Thus, we derive the mean neutral hydrogen fraction $x_{\rm H\,I}$ along the synthetic LOS characterized by $W_{\rm max} \epsilon\, [51\,\text{Å} \pm {\rm d}\,W]$ for $F_{\rm th}^{\rm obs} = 0.30 \times 10^{-18}$ erg s^{-1} cm^{-2} Å^{-1} and $W_{\rm max} \epsilon\, [78\,\text{Å} \pm {\rm d}\,W]$ for $F_{\rm th}^{\rm obs} = 0.35 \times 10^{-18}$ erg s^{-1} cm^{-2} Å^{-1}. We find that the observed LGW in the GRB 050904 afterglow spectrum are consistent with $x_{\rm H\,I} = 6.4 \pm 0.3 \times 10^{-5}$.

6 CONCLUSIONS

We have proposed to investigate cosmic reionization using absorption-line spectra of high-z GRB afterglows. The evolution of the LGW as a function of the flux threshold $F_{\rm th}$ used to define gaps shows marked differences in the two reionization models favoured by present data. In particular, (i) the LGW is typically ~2 times wider in the LRM than in the ERM, for a fixed $F_{\rm th}$; (ii) the difference between ERM and LRM in terms of $(W_{\rm max}, F_{\rm th})$ increases with z; (iii) an overall shift towards larger $W_{\rm max}$ values for a fixed $F_{\rm th}$ is found in both models towards higher redshifts. This analysis has shown that we can robustly distinguish among different reionization histories: improved results can be obtained if data are collected promptly after burst detection and by using GRBs at the highest available redshifts.

A direct comparison of the model with data can be carried on in terms of the probability to find the largest gap in a given width range for burst afterglows at $z = z_{\rm GRB}$. When applied to the only known GRB at $z > 6$, i.e. GRB 050904 at $z_{\rm GRB} = 6.29$, a clear indication is obtained that reionization must have occurred well before $z = 6$.

We find that the observed LGW in the GRB 050904 afterglow spectrum are consistent with $x_{\rm H\,I} = 6.4 \pm 0.3 \times 10^{-5}$. This result is in agreement with previous measurements by Totani et al. (2006), who find that $x_{\rm H\,I}$ is bound to be $x_{\rm H\,I} < 0.17$ (<0.6) at 68 per cent (95 per cent) CL.

Some gaps/peaks in absorption spectra could be due to DLAs/H II regions intervening along the LOS towards the background source (e.g. the DLAs/transverse proximity effect detection by Totani et al. 2006/G07). Such contaminants could affect neutral hydrogen measurements, if the foreground sources are not properly removed.

In this work, we have applied the gap statistics to the GRB 050904 observed flux. However, the same analysis can be done by using the transmitted flux $F_{\rm obs}/F(\nu)$, i.e. normalizing the observed flux to the continuum. Following this approach, we provide useful plots (Fig. 2) which allow a straightforward comparison between our model results and future observations of $z > 6$ GRBs afterglow spectra.

It is worth noting that the gap statistics with a variable flux threshold can be readily applied to other background sources, as QSOs. We plan to apply this analysis to the Fan et al. (2006) data, thus improving the results obtained by G07. The advantage of varying the flux threshold is that this technique allows to study the response of the transmitted flux both to the high- and low-end tail of the IGM density field. In fact, high (low) $F_{\rm th}$ values probe regions corresponding to low (high) overdensities.

In spite of the fact that QSO data are presently more abundant, GRBs are expected to be found at higher redshift, as they should result from the death of (early) massive stars (e.g. Abel, Bryan & Norman 2002; Schneider, Guetta & Ferrara 2002). Larger samples of GRB afterglow spectra at $z \geq 6$, likely available in near future, will allow a statistically significant analysis and possibly to reconstruct the cosmic reionization history. At redshifts approaching reionization epoch, gaps in afterglow absorption spectra are expected to become as large as the spectral region between the Lyα and Lyβ emission lines, thus obscuring completely the GRBs optical counterpart.

ACKNOWLEDGMENTS

We thank E. Pian for providing useful instrumental data, G. Chincarini, D. Malesani and G. Tagliaferri for stimulating discussions about GRB afterglows and *Swift* data, Z. Haiman for enlightening comments and the referee, J. Schaye, for constructive criticism.

REFERENCES

Abel T., Bryan G. L., Norman M. L., 2002, Sci, 295, 93
Becker G. D., Rauch M., Sargent W. L. W., 2007, ApJ, 662, 72
Bromm V., Loeb A., 2006, ApJ, 642, 382
Campana S., Tagliaferri G., Malesani D., Stella L., D' Avanzo P., Chincarini G., Covino S., 2007, A&A, 464, L25
Choudhury T. R., Ferrara A., 2006, MNRAS, 371, L55
Daigne F., Rossi E. M., Mochkovitch R., 2006, MNRAS, 372, 1034
Fan X., 2006, New Astron. Rev., 50, 665
Fan X. et al., 2006, AJ, 132, 117
Gallerani S., Choudhury T. R., Ferrara A., 2006, MNRAS, 370, 1401 (G06)
Gallerani S., Ferrara A., Fan X., Choudhury T. R., 2007, MNRAS, 386, 359 (G07)
Gehrels N. et al., 2004, ApJ, 611, 1005
Haislip J. B. et al., 2006, Nat, 440, 181
Hinshaw G. et al., 2007, ApJS, 170, 288
Kawai N. et al., 2006, Nat, 440, 184
Natarajan P., Albanna B., Hjorth J., Ramirez-Ruiz E., Tarvir N., Wijers R., 2005, MNRAS, 364, L8
Page M. J. et al., 2007, ApJS, 170, 335
Paschos P., Norman M. L., 2005, ApJ, 620, L9
Ruiz-Velasco A. E. et al., 2007, ApJ, 669, 1
Salvaterra R., Chincarini G., 2007, ApJ, 656, L49
Salvaterra R., Campana S., Chincarini G., Tagliaferri G., Covino S., 2007, MNRAS, 380, L45
Salvaterra R., Campana S., Chincarini G., Covino S., Tagliaferri G., 2008, MNRAS, 385, 189
Schneider R., Guetta D., Ferrara A., 2002, MNRAS, 334, 173
Spergel D. N. et al., 2007, ApJS, 170, 377
Starling R. L. C., Wijers R. A. M. J., Hughes M. A., Tanvir N. R., Vreeswijk P. M., Rol E., Salamanca I., 2005, MNRAS, 360, 305
Tagliaferri G. et al., 2005, A&A, 443, L1
Totani T., Kawai N., Kosugi G., Aoki K., Yamada T., Iye M., Ohta K., Hattori T., 2006, PASJ, 58, 485
Vreeswijk P. M. et al., 2007, A&A, 468, 83

This paper has been typeset from a TEX/LATEX file prepared by the author.